Critical Ignition in Detonation Cells due to Expansion Cooling

K. Cheevers, R. Murugesan, F. Giroux, W. Morin, A.-A. Dion-Dallaire, M. I. Radulescu
University of Ottawa
Ottawa, Ontario, Canada

1 Introduction

Gaseous detonation waves are characterized by a cellular structure. During a cell cycle, the lead shock continuously decays, and it is re-amplified during triple shock reflections. The present study addresses the laminar-like ignition behind the decaying lead shock of cellular detonations, taking into consideration the gasdynamic expansion of the fluid particles behind the decaying curved lead shock.

The effect of gasdynamic expansion on ignition in detonation cells was first studied by Lundstrom and Oppenheim [1] for H_2-O_2-N_2 detonations. They fitted the shock decay to a Taylor-Sedov profile. Using blast wave theory, they inferred the gasdynamic expansion felt by fluid particles undergoing ignition behind the leading shock. They assumed induction kinetics derived from shock tube experiments. They found that ignition is quenched during the lead shock decay approximately half way in the cellular structure due to expansion cooling. Shepherd and co-workers also investigated the possibility of ignition quenching in detonation cells, by applying their Critical Decay Rate model developed by Eckett et al. [2] to the shock decay in cells. They neglected the effect of curvature and assumed a single step reaction tuned to reproduce ignition delays computed with more realistic chemical models. These authors also found that ignition may be quenched in numerical simulations of detonation cells for model parameters [3]. Kiyanda et al. subsequently applied an ignition analysis along the particle paths of detonations under some simplifying assumptions in CH_4-O_2 detonations and also concluded that ignition behind the leading shock may be quenched after the first half of the cycle [4]. In spite of differences in modelling assumptions, these studies thus suggest that ignition behind the leading shock of detonations can be quenched by gasdynamic expansions. In experiments, the gas survives quenching by either gasdynamic heating by transverse shocks and/or turbulent mixing with reaction products [5].

In the present study, we revisit the analysis of expansion cooling behind the lead shock of detonations by addressing some of the shortcomings of the previous studies. We include the effect of shock wave curvature, neglected in the analysis of Shepherd et al., and we conduct ignition calculations using state-of-the-art chemical modelling. We study two reactive mixtures, namely $CH_4 + 2O_2$ and $2H_2+O_2 + 7Ar$, which represent the two extremes of cellular regularity and sensitivity of the ignition delay to temperature changes. The latter mixture is known to have the most regular detonation structure. We wish to comment whether ignition quenching by gasdynamic expansion is universal for all cellular detonations. The experiments are performed within a thin rectangular shock tube, allowing a quasi-two-dimensional analysis which neglects the three-dimensional effects present during a cellular detonation.

Correspondence to: kevin.cheevers@uottawa.ca

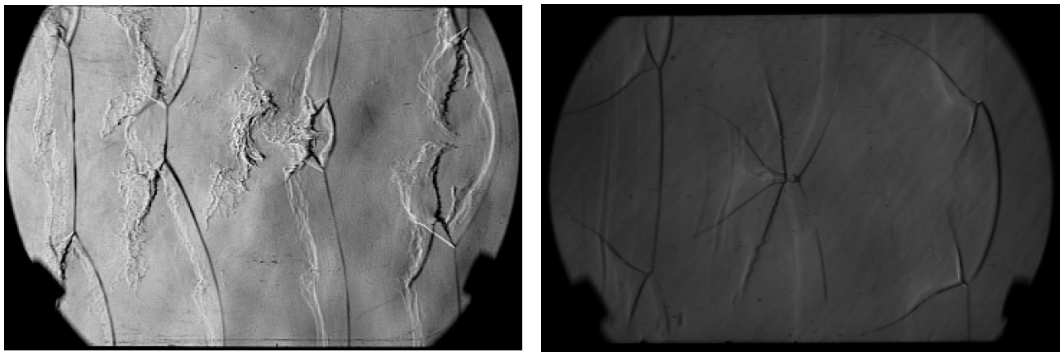

Figure 1: Evolution over multiple frames of the shock's cellular structure taken by Z-type Schlieren photography. Left : CH_4 + $2O_2$, Right : $2H_2$+O_2 + 7Ar

2 Experimental Method

Detonation experiments were performed in a shock tube with a 203 mm by 19 mm rectangular cross-section. Mixtures of CH_4 + $2O_2$ and $2H_2$+O_2 + 7Ar were studied under conditions where a single cell was observed across the channel height, as shown in Fig. 1. Experimental conditions are listed in Table 1. A high-speed camera, placed within a Z-type Schlieren configuration, was used to capture the evolution of the experiment.

Each image was analyzed using ImageJ in order to record the position of the shock and the onset of exothermicity behind the shock. These were measured along the detonation cell's centreline as well as along both the top and bottom walls. The radius of curvature of the lead shock was measured at the aforementioned locations by using various curve-fitting methods of the shock locus. Since the images did not provide an entire continuous cell cycle, the shock decay at the end of the cell cycle (centreline prior to triple point collisions), at the beginning (centreline after triple point collisions) and at its intermediate stages (top and bottom walls) were combined to reconstruct the desired signal.

Table 1: Experimental Test Conditions

Mixture	p_0	T_0	Interframe Time
CH_4 + $2O_2$	3.5 kPa	293 K	11.53 μs
$2H_2$ + O_2 + 7Ar	4.1 kPa	293 K	12.91 μs

3 Ignition calculations behind non-steady shocks

Given the experimentally determined shock decay and shock curvature, the characteristic rate of expansion along a particle path can be derived from the conservation laws following similar arguments as used by Fickett and Davis to derive their shock change equations [6], yielding

$$\frac{1}{\rho}\frac{D\rho}{Dt} = \frac{-\dot{\sigma} + u\kappa M^2 + \frac{1}{\rho c^2}\left(\frac{dp}{dt}\right)_S \left(1 + \rho_0(D-u_0)\left(\frac{du}{dp}\right)_H\right)}{1-M^2} \tag{1}$$

In this equation, the term $\dot{\sigma}$ denotes the thermicity behind the lead shock ($\dot{\sigma} = 0$ in the induction zone), κ denotes the shock curvature, M is the flow Mach number behind the leading shock, D the shock speed, ρ is the density behind the shock, and c and u are respectively the sound speed and the flow speed behind the

lead shock. ρ_0 and u_0 are the density and flow speed ahead of the lead shock. The term $\left(\frac{du}{dp}\right)_H$ represents the variation of the flow speed behind the shock with the shock pressure, which is a property of the shock Hugoniot. The term $\left(\frac{dp}{dt}\right)_S$ is the decay of shock pressure with time.

This relation can be used directly given local values of shock curvature κ and shock strength decay rate $\left(\frac{dp}{dt}\right)_S$, with the gas specific terms evaluated from thermo-chemical properties leading to the shock Hugoniot. A simpler, yet as accurate model can be also obtained for strong shocks in ideal gases, yielding

$$\frac{1}{\rho}\frac{D\rho}{Dt} = \frac{6}{\gamma+1}\frac{\dot{D}}{D} + 2\kappa D\frac{\gamma-1}{(\gamma+1)^2} \tag{2}$$

The first term on the right hand side is the shock unsteadiness effect on volumetric expansion, while the last term is the role of shock wave curvature. Note that only the unsteady term appears in the CDR model of Shepherd and co-workers.

With the Lagrangian expansion term given in terms of the shock dynamics from the shock change equations, the ignition calculations assume that this volumetric expansion rate remains constant during the subsequent ignition process. This assumption of constant characteristic volumetric expansion, also assumed in the Shepherd's CDR model [2] renders the ignition analysis a local one in the vicinity of the lead shock. Note that alternate forms of expansion rate would yield very similar results [7].

The 0D ignition calculations were performed for a reactor with prescribed volume changes. The calculations were performed using Cantera [8] to integrate the kinetics given by the San Diego mechanism [9].

4 Results

The shock speed of the analyzed experimental frames decays with the cyclic distance, and an exponential curve fit is applied to the measured data [10]. The data points and the fitted curve are shown in Figure 2. The shock speed is found to be within the range of Mach 5 to 7 for the methane-oxygen mixture and of Mach 3 to 5 for the hydrogen-oxygen-argon mixture. The use of the strong shock change equation is thus justifiable for the range of shock speeds studied for both experimental mixtures.

Small variations in the measurement of the radius of the lead shock lead to visible variations in the curvature values obtained due to the sensitivity of the reciprocal function to fluctuations of the denominator. The values measured at the beginning of the cellular cycle have a tendency to diverge from the fitted curve due to this sensitivity to smaller radii. Despite this, the convergence of the remainder of the cycle with an exponential curve leads to the conclusion that the curvature decreases exponentially over a cellular cycle, as seen in Figure 3.

To study the thickening of the induction zone, x-t diagrams were constructed, seen in Figure 4. The x-t diagrams show the experimental and calculated ignition fronts alongside the lead shock and particle paths. The experimental and calculated ignition fronts are found to be very similar for the hydrogen-oxygen mixture, however in the methane-oxygen mixture differences appear between these two curves. The calculated ignition front is very similar to the measured experimental ignition front for the first half of the cellular cycle, however it differs within the second portion of the cellular cycle. The acceleration of the lead shock decay is not transmitted to the reaction front, thus terms representative of additional losses are required for a larger deceleration of the calculated ignition front. The particle paths studied have the behaviour of crossing

the lead shock and decelerating until reaching the experimental ignition front, near which ignition occurs. Figure 4 shows an increasing distance between the ignition point of each subsequent particle path and the lead shock due to the thickening of the induction zone with the weakening of the lead shock.

Studying the ignition time in more detail, one can obtain the critical ignition limit within the cycle, taken as the particle path after which the shocked mixture is quenched by the volumetric expansion, if it were to be maintained at the same characteristic rate. This ignition limit represents the point at which the induction zone begins to noticeably thicken, seen qualitatively when looking at the sequence of experimental frames in Figure 1. Figure 5 shows that this critical ignition condition occurs in both mixtures within the first half of the cellular cycle, and earlier for the methane system. This is attributed to much higher sensitivity of the induction kinetics in methane.

Referring to Figure 1, one notices the presence of various reaction mechanisms taking place past this critical ignition limit throughout the later portion of the cellular cycle. In the hydrogen system, the gas reacts behind the transverse shocks, which further compress the post-shock gases to promote the formation of a transverse reaction front. In the methane system, the unburned gases are consumed by turbulent flames on the edges of the non-burned pockets, once these are isolated from the front after triple shock collisions [11].

In previous work, Shepherd and co-workers have neglected the effects of curvature on the expansion, since they were interested in shocks approximated by Taylor-Sedov blast waves. In the present study, the real dynamics of the lead shock in the cells can be analyzed in order to determine the relative importance of curvature and unsteadiness appearing in (1) or (2). Figure 6 shows the ratio of these two terms for the two mixtures investigated. One notices that the curvature effects are of comparable order of magnitude to the unsteadiness effects. For both strongly and weakly sensitive mixtures, the curvature effects present are roughly half that of the unsteadiness effects at the beginning of the cycle. The ratio between the competing effects significantly drops near the critical ignition limit, which suggests that the notable change in curvature over the cellular cycle has an important role in the quenching of the shocked mixture past the critical ignition limit. By the end of the cellular cycle, the curvature effects have decreased to an order of magnitude smaller than the unsteadiness effects present.

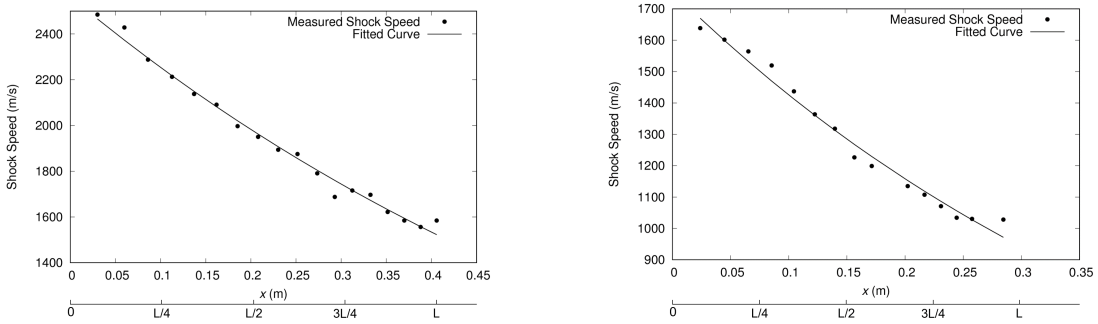

Figure 2: Speed of the leading shock measured over a cellular cycle, shown alongside an exponential trend-line. Left : $CH_4 + 2O_2$, Right : $2H_2$+O_2 + 7Ar

5 Concluding Remarks

Expansion cooling was studied by evaluating both the shock decay and the change in curvature of the lead shock over a cyclic detonation cell. The effect of the lead shock's curvature was expressed alongside the shock decay term in a shock change equation to link the quiescent state to the post-shock state and find the

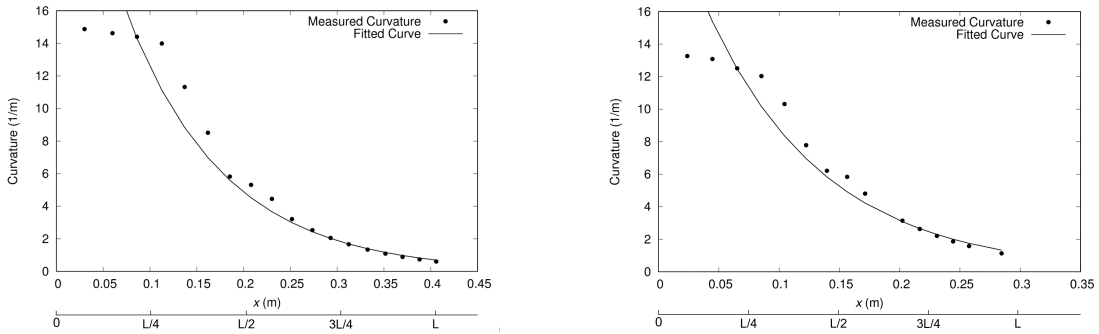

Figure 3: Curvature measurements over a cellular cycle, shown alongside an exponential trendline. Left : $CH_4 + 2O_2$, Right : $2H_2$+O_2 + 7Ar

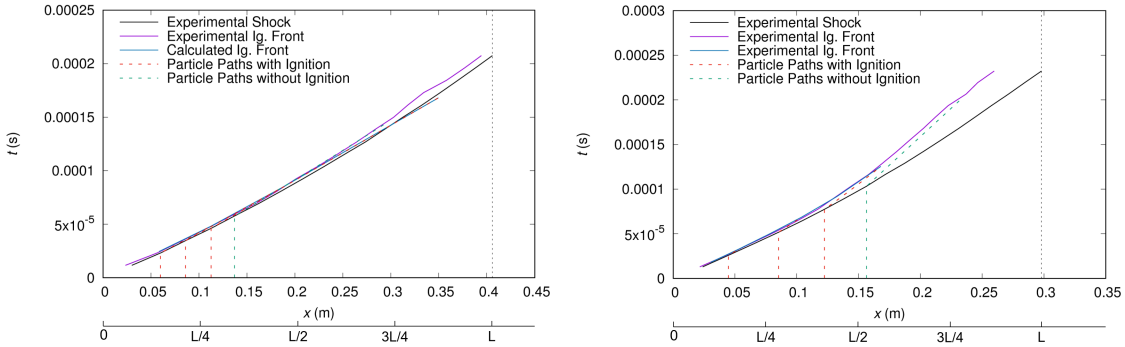

Figure 4: x-t diagram of the lead shock, the onset of exothermicity, and with select particle paths. Left : $CH_4 + 2O_2$, Right : $2H_2$+O_2 + 7Ar

expansion rate along various particle paths. This expansion rate was coupled with full chemistry combustion simulations to find the particle path along which the ignition process is quenched. Such critical ignition was observed in both strongly and weakly sensitive mixtures, suggesting it is universal for cellular detonation dynamics. The curvature effects on the post-shock exothermic reactions was found to be as important as the non-steady effects prior to the critical ignition limit, at which point the curvature effects decrease to become small compared to the unsteadiness effects.

References

[1] E. A. Lundstorm and A. K. Oppenheim, "On the influence of non-steadiness on the thickness of the detonation wave," *Proc. Roy. Soc.*, vol. 310, pp. 463–478, 1969.

[2] C. A. Eckett, J. J. Quirk, and J. E. Shepherd, "The role of unsteadiness in direct initiation of gaseous detonations," *Journal of Fluid Mechanics*, vol. 421, pp. 147–183, 2000.

[3] J. Austin, *The role of instability in gaseous detonation*. PhD thesis, California Institute of Technology, Pasadena, California, 2003.

[4] C. J. Kiyanda, A. J. Higgins, and J. H. S. Lee, *Photographic study of the two-dimensional dynamics of irregular detonation waves*. Montreal, QC, Canada: 20th Itntl Colloqium on Dynamics of Explosions and Reactive Systems, 2005.

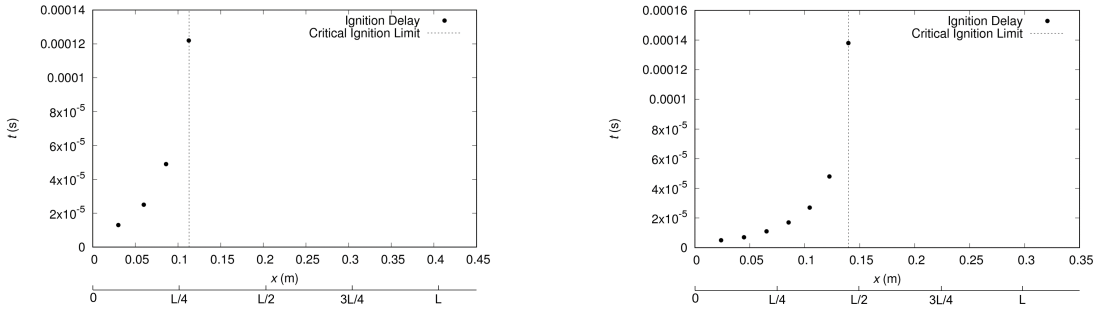

Figure 5: Ignition delays throughout a cycle, shown alongside the asymptotic ignition limit for the critical ignition case. Left : CH_4 + $2O_2$, Right : $2H_2$+O_2 + 7Ar

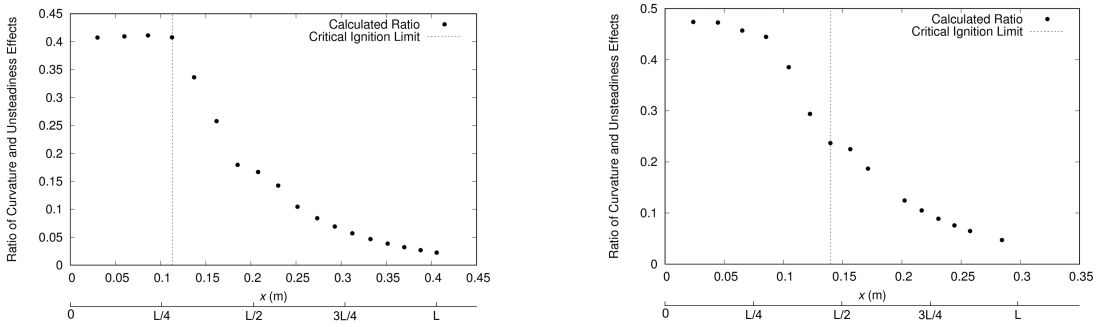

Figure 6: Ratio between the curvature and the unsteadiness terms present in the shock change equation, over a cellular cycle. Left : CH_4 + $2O_2$, Right : $2H_2$+O_2 + 7Ar

[5] M. Radulescu, "A detonation paradox: Why inviscid detonation simulations predict the incorrect trend for the role of instability in gaseous cellular detonations?," *Combustion and Flame*, vol. 195, pp. 151–162, 2018.

[6] W. Fickett and W. C. Davis, *Detonation theory and experiment*. Dover Publication Inc., 1979.

[7] M. I. Radulescu and B. M. Maxwell, "Critical ignition in rapidly expanding self-similar flows," *Phys. Fluids*, vol. 22, p. 066101, 2010.

[8] D. G. Goodwin, H. K. Moffat, and R. L. Speth, "Cantera: An object-oriented software toolkit for chemical kinetics, thermodynamics, and transport processes." http://www.cantera.org, 2017. Version 2.3.0.

[9] F. A. Williams, "Chemical-Kinetic Mechanisms for Combustion Applications, San Diego Mechanism web page, Mechanical and Aerospace Engineering (Combustion Research), University of California at San Diego (http://combustion.ucsd.edu)," 2014.

[10] S. I. Jackson, C. Chiquete, and M. Short, "An intrinsic velocitycurvatureacceleration relationship for weakly unstable gaseous detonations," *Proceedings of the Combustion Institute*, 2018.

[11] B. Maxwell, R. Bhattacharjee, S. Lau-Chapdelaine, S. Falle, G. J. Sharpe, and M. I. Radulescu, "Influence of turbulent fluctuations on detonation propagation," *Journal of Fluid Mechanics*, vol. 818, pp. 646–696, 2017.